



Preparation and optical properties of CdS/Epoxy nanocomposites

F. A. Kasim¹, M. A. Mahdi¹, J. J. Hassan¹, S. K. J. Al-Ani^{2,*}, S. J. Kasim¹

¹Physics Department, College of Science, Basra University, Basra-IRAQ.

²Physics Department, College of Science, Baghdad University- Baghdad-IRAQ.

Received 18 July 2010; Revised 7 Jan. 2011; Accepted 6 May 2011

Abstract

The CdS/Epoxy nanocomposites (5%,20% CdS ratio) were prepared by *in situ* method using cadmium acetate and thiourea as a source of Cd²⁺ and S²⁻ ions to form CdS nanoparticles in epoxy matrix solution. The X-ray diffraction patterns show that crystallinity of the samples was decreased with increase in the CdS ratio in the nanocomposites. The FTIR and the UV-Visible absorption spectra were performed for prepared samples to determine the assignment bands and the absorption edges respectively. The effective mass model has been used to calculate the diameters of the CdS nanoparticles and they were 4.5 and 4.8 nm for 5% and 20% CdS+ Epoxy respectively. The photoluminescence spectra of CdS/Epoxy showed two emission peaks, the first one varies from 470 to 480 nm for 5% and 20% CdS+ Epoxy respectively, due to energy gap variation with particle size, and the second one at 600 nm bears the signature of the red emission (Lambe_Klick model) which could be due to the recombination of electrons trapped at sulfur (S) vacancies with valence-band-free holes.

Keywords: CdS; Epoxy; Nanocomposites; XRD.

PACS: 62.23.Pq;78.67.-n; 78.55.-m; 78.30.-j.

1. Introduction

In recent years, nanotechnology progress has been achieved in the synthesis of the various types of polymer-nanocomposites and understanding the basic principles which determine their physical and chemical properties. Polymer- semiconductor nanocomposites are new generations of hybrid organic-inorganic materials which are composed by semiconductor nanoparticles (inorganic) dispersed within a polymer matrix (organic) forming polymer - semiconductor nanocomposites[1,2]. Nanoparticles are distinguished from the bulk due to their high surface to volume ratio of nanoparticles that causes the structural and electronic changes that in turn, induce other properties to become different from that of the bulk [3]. The polymer-nanocomposites have gained much interest due to the remarkable changes in their properties such as optical, electrical, mechanical, thermal and magnetic compared to pure organic polymers [4-7].

The II-VI group of semiconductors (CdS, ZnS, PbS,...etc) can be formed with polymer to produce polymer nanocomposites materials. These II-VI sulfides used in wide range of applications in various optoelectronic devices[8-10]. Among the II-VI Semiconductors, CdS is a representative material with many applications such as large area

*) For Correspondence; Email: salwan_kamal@yahoo.com

electronic devices and solar cells, because it has a wide direct band gap (2.42 eV)[11,12]. Transparent epoxy resins have been most frequently employed in standard light emitting diode (LED) technology as packaging materials because of their excellent transparency, high-glass transition temperature, low-water absorption and standard processability [13].

There are two important advantages for CdS-polymer nanocomposites, the first that the polymer matrix can make nanometer scale CdS clusters and led to improving of the stability, dispersion and mechanical strength of the materials. Another advantage is that the surface of the CdS nanoparticles could be modified by the polymeric matrix via the interactions between the two components.

In this work, CdS/Epoxy nanocomposites were prepared by incorporating different ratio of CdS nanoparticles into an epoxy matrix and the optical properties of the nanocomposites were characterized by the FTIR, UV-Visible and Photoluminescence (PL) spectra.

2. Experimental

2.1 Materials

The diglycidyl ether of bisphenol-A (DGEBA), transparent epoxy resin (EPLU-200A) used as host material, diethylenetriamine (DETA) used as curing agent are commercial available. The chemical structures of EPLU-200A and DETA are shown in Fig. 1. Other chemicals, N,N-dimethylformamide (DMF), cadmium acetate Cd(Ac)₂ and thiourea were also used to prepare the samples.

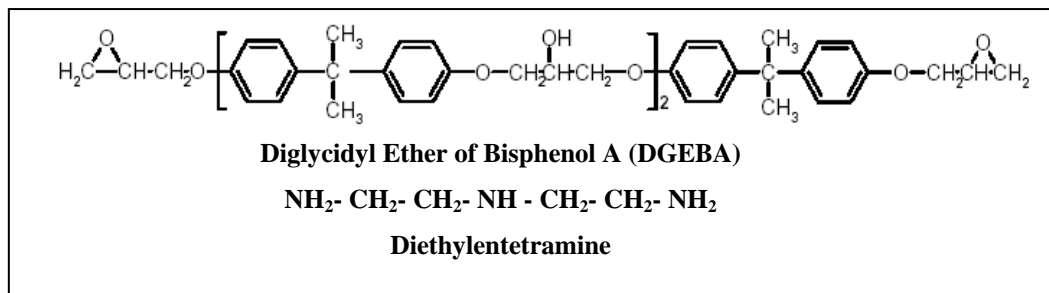


Fig. 1: The chemical structure of monomers.

2.2 The mechanism of the epoxy curing reaction

In general terms, the mechanism of the epoxy curing reaction using diamine hardeners can be obtained. The reaction consists in the epoxy ring, opening by the primary amine reactive group generating secondary amines and hydroxyl groups. Subsequently, as the secondary amines are generated they can react with the epoxy rings at the same time as primary amines to yield tertiary amines and hydroxyl groups as shown in Fig. 2. Therefore, as the curing reaction proceeds, the OH⁻ concentration must increase in proportion to the disappearance of the epoxy groups and the concentration of primary amines will continuously decrease. [14]

2.3 The preparation of the CdS/Epoxy nanocomposites

The transparent epoxy resin (EPLU-200A) (2.4gm) was dissolved in 20ml DMF, and then sufficient quantity of cadmium acetate $\text{Cd}(\text{Ac})_2$ was added and mixed together in a closed beaker by using hot plate magnetic stirrer for 15min. Similarly, diethylenetriamine (DETA) (0.8gm) and thiourea ($\text{Cd}(\text{Ac})_2/\text{thiourea}=1.2$) were dissolved in 20ml DMF and mixed in another beaker with stirrer for 15 min at a temperature of $T=70^\circ\text{C}$. A clear solution of cadmium acetate with Epoxy EPLU-200A, and a clear solution of thiourea with diethylenetriamine were then mixed in a closed beaker with stirrer (30 min, at T of 70°C). The CdS concentration in the polymer could be about 5wt % and 20wt %.

Finally, the homogenous viscous liquid of an orange color was obtained. The homogenous viscous liquid was then poured in a plastic mould in oven at $T=50^\circ\text{C}$ for 24 min to evaporate the solvent and then the post curing was performed at $T=130^\circ\text{C}$ for 1h. The thicknesses of samples were (430-450 μm) and the yellowness of samples were increased at CdS ratio increased (Fig. 3). CdS nanoparticles dispersed in epoxy matrix to produce nanocomposites as shown in figure 4, consequently, the so-called nanoparticle filled polymers sometimes contain a number of loosened clusters of particles and exhibit properties even worse than conventional particle/polymer systems.

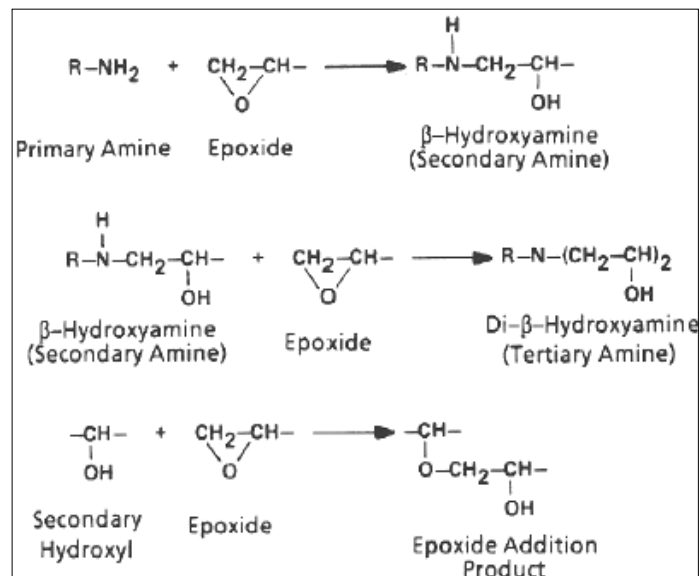


Fig. 2: Crosslinking reaction between the epoxide ring and the primary amine.

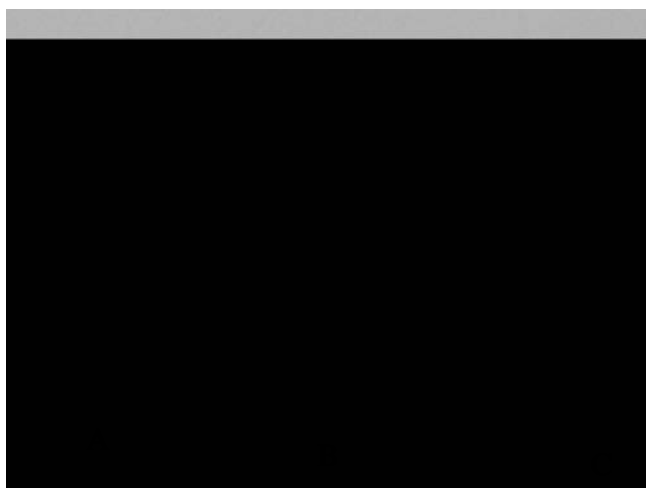


Fig. 3: Photographs of A: Pure epoxy polymer, B: CdS(5%)/epoxy and C: CdS(20%)/ epoxy nanocomposites

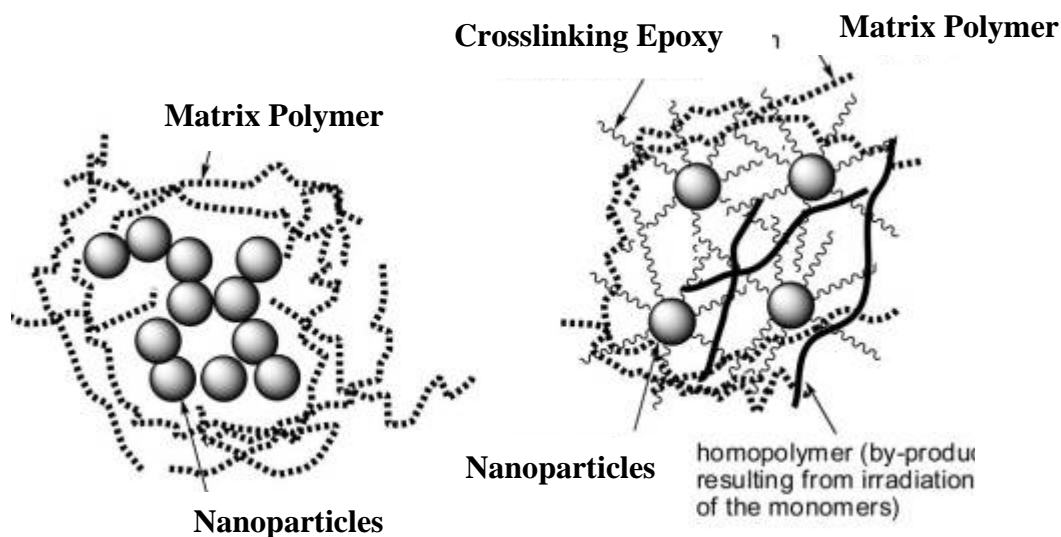


Fig. 4: Agglomerated CdS nanoparticles dispersed in Epoxy matrix

2.4 The characterization techniques

The structural properties of CdS/Epoxy nanocomposites samples were studied by using X-ray diffraction(XRD) method (system type: X'Pert Pro MPD by PANalytical company) where the target was $\text{CuK}\alpha$ radiation ($\lambda= 1.54 \text{ \AA}$) in the range of $2\theta=(10-60)^\circ$.

The Fourier Transform Infrared (FTIR) spectra of the CdS/Epoxy nanocomposites were performed using spectrophotometer (type Shimadzu 800). The FTIR spectral region was recorded in the range ($500 - 4000 \text{ cm}^{-1}$). The optical properties of the transparent-inorganic CdS/Epoxy nanocomposites were studied using a UV-visible spectrophotometer (model Thermo Spectronic) and the absorbance spectra were scanned in the range of 190–1100 nm with a 1 nm interval. The photoluminescence (PL) spectra were acquired by

Perkin-Elmer LS1 fluorescence spectrometer at room temperature operating with excited wavelength (λ) of 302 nm.

3. Results and discussions

3.1 The FTIR of the CdS/Epoxy nanocomposites

Fig. 5 shows the FTIR spectra of the Epoxy and CdS/Epoxy nanocomposite before curing process. The main IR absorption bands of the CdS/Epoxy nanocomposites were assigned the specific groups as from reference [15] and presented in Table 1.

The representative FTIR spectra of the CdS/Epoxy nanocomposite has a significant change in the absorption bands and could not easily observed. These changes belong to the differences between the neat Epoxy and the nanocomposites[16]. The shift in absorption bands of CdS/Epoxy with respect to neat Epoxy belong to CdS nanoparticles which effect on it.

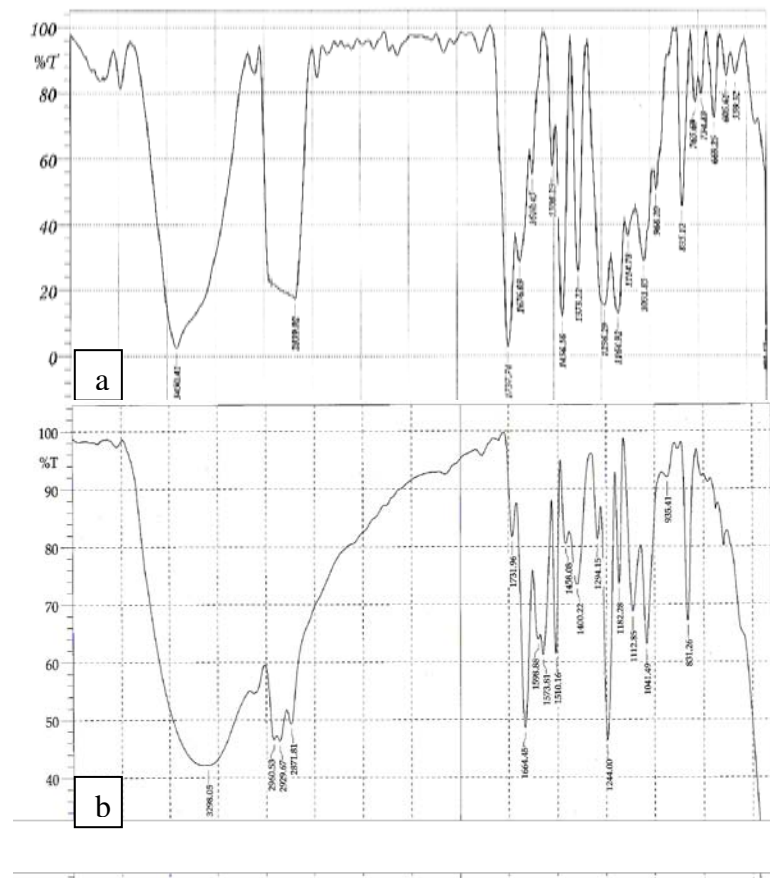


Fig. 5: The FTIR spectra of a: Epoxy resin and b: CdS/Epoxy nanocomposite before curing process.

Table 1: The main infrared absorption bands of the Epoxy and CdS/Epoxy nanocomposite. s: strong; m: medium, w: weak

Epoxy Band (cm^{-1})	CdS/Epoxy Band (cm^{-1})	Assignment
3450	3298	O—H stretching
2970, 2871	2960, 2929, 2871	Aliphatic C—H stretching
1737, 1676	1731, 1664	C=O stretching
1610 _m , 1508 _m	1598 _m , 15731 _w , 1510 _s	Aromatic ring
1456 _s , 1373 _s	1458 _w , 1400 _m	CH ₃ asymmetrical bending
1236 _m	1244 _s , 1294 _m	C—O bonds stretching
1164 _m , 1114 _w , 1031 _m	1182 _m , 1112 _w , 1041 _m	Ar—O—R asymmetrical bending
968	935	Epoxy ring: C—C bond contracting while both C—O bond stretch
835	831	Aromatic ring bending

3.2 The X-Ray diffraction of the CdS/Epoxy nanocomposites

Fig. 6 displays the XRD patterns of the neat epoxy and the CdS/Epoxy nanocomposites of (5% and 20%) CdS. The samples recorded a single broad peak focused at about $2\theta=20^\circ$. No significant difference between the reference neat epoxy film and the 5% CdS nanocomposites was found because of the largely amorphous structure of Epoxy. In the case of the 20% CdS nanocomposite sample the broad amorphous peak that centered at $2\theta=20^\circ$ was disappeared. Again, there no noticeable difference between the reference Epoxy and the CdS nanocomposite with the increase of CdS and it had not specified any crystalline structure. This confirms the amorphous nature of the materials (Epoxy). The Epoxy is largely amorphous so, the CdS nanoparticles diffraction peaks were did not show due to the small particles sizes.

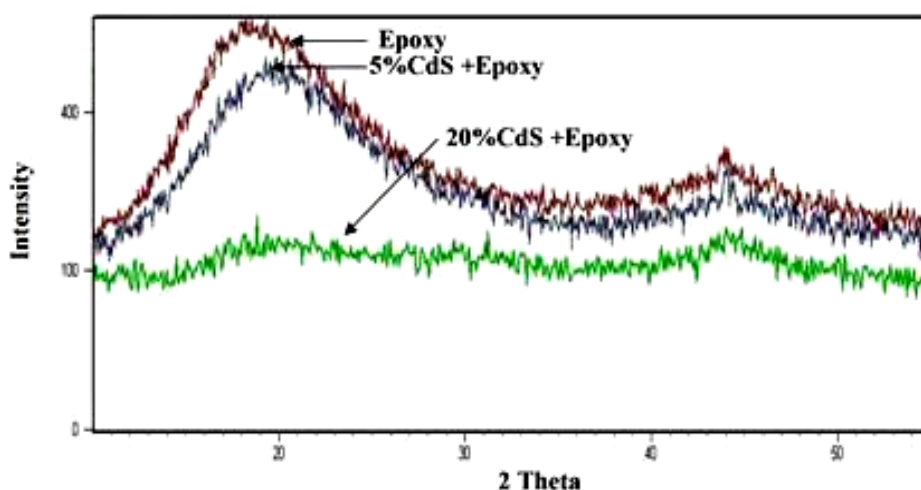


Fig. 6: The X-ray diffraction pattern of the CdS/Epoxy nanocomposite samples

3.3 The optical properties of the CdS/Epoxy nanocomposites

The absorption spectra of the neat Epoxy and the CdS/Epoxy nanocomposites films are shown in Fig.7. All spectra show a blue shifted absorption onset with respect to the 516 nm of the bulk CdS semiconductor, proving the presence of the nanostructured CdS. The cut-off wavelength has been estimated from the intersection of the tangent line of the peak with the wavelength axis. This wavelength is used to determine the band gap of the CdS nanoparticles by using the relationship:

$$E_g^* = \frac{hc}{\lambda_c} \quad (1)$$

Where λ_c = wavelength absorbed by the sample and c is the speed of light.

The particle size can be calculated from the UV-Vis absorption spectrum using the following expression derived from the effective mass model or Brus equation [17]:

$$E_g^* = E_g^{bulk} + \frac{\hbar^2 \pi^2}{2r^2} \left(\frac{1}{m_e^*} + \frac{1}{m_h^*} \right) - \frac{1.8e^2}{4\pi\epsilon\epsilon_0 r} - \frac{0.124e^4}{\hbar^2 (4\pi\epsilon\epsilon_0)^2} \left(\frac{1}{m_e^*} + \frac{1}{m_h^*} \right)^{-1} \quad (2)$$

where E_g^* is the energy band gap of the nanoparticle, which will be determined from the UV-Visible absorbance spectrum, E_g^{bulk} is the energy band gap of the bulk CdS at room temperature, which has the value of 2.42 eV, h is the Planck's constant, r particle radius (m), m_e mass of a free electron, m_e^* (0.19 m_e) and m_h^* (0.8 m_e) are the effective masses of the electron in the conduction band and of the hole in the valence band respectively, e the electron charge, ϵ_0 the permittivity of free space and ϵ relative permittivity of CdS. The particles size have been calculated and listed in Table 2.

Table 2: The band edge onset of the nanocomposites

Samples	Band edge onset (nm)	E_g (eV)	Particles size (nm)
5% CdS+Epoxy	462	2.68	4.5
20% CdS+Epoxy	470	2.63	4.8

According to data in Table 2, the absorption edges of the CdS nanocomposites shift to higher energy as the size of CdS nanoparticles is reduced. This blue shift in the energy gap between the valence band and the conduction band of the CdS nanocomposites (Fig. 7) is an experimental evidence for a quantum confinement that corresponding to an increase in the absorption edge and consequently the energy gap of the CdS-epoxy nanocomposites. Our results are in agreement with other nanocomposites CdS-polymer nanocomposites [18].

Wang and his team [19] noted that the absorption edge of CdS in PVA matrix decreased to short wavelength at cadmium acetate decreased which mean the smaller CdS nanoparticles were produced at a small amount of Cd salt.

The samples which are prepared have a high transmission (65%) in the visible spectra (after $\lambda = 470$ nm) for the epoxy and the (5wt.%) CdS in the Epoxy, but becomes of low transmittance for the (20wt.%) CdS in the Epoxy.

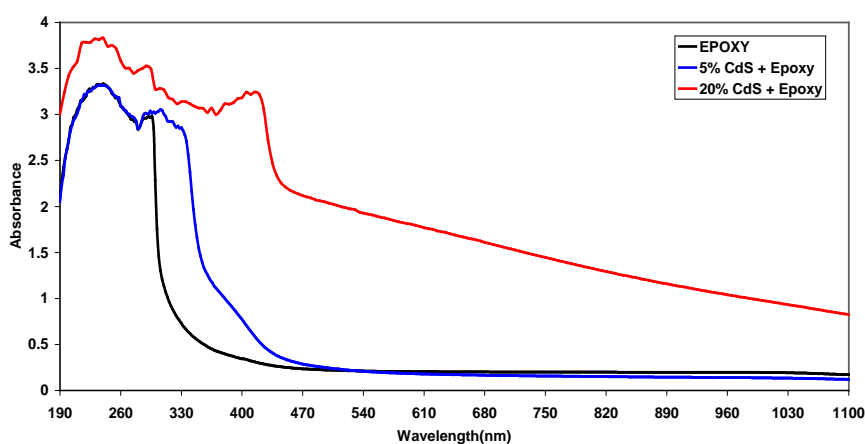


Fig. 7: The absorption spectra of CdS/Epoxy nanocomposites

3.4 Photoluminescence spectra

In photoluminescence, electrons in a material transfer to allowed excited quantum states upon absorption of a higher energy photon. Normally, two emissions can be obtained from nanocrystalline semiconductor: one is the sharp excitonic emission located near the absorption edge and another broad emission at longer wavelength due to surface states or defects [20]. Recombination of the electron and hole results in emission of a photon (i.e. radiative recombination leads to PL). Some radiative events from band edge, defects and nonradiative processes are shown in Fig. 8 [20].

Figure 9 shows the photoluminescence spectra of CdS/Epoxy nanocomposites. The PL peak shifted toward red wavelength (from 470 to 480nm) at CdS percent ratio increased from 5 to 20% which mean decreased in optical band gap due to increasing in particle size. The sample which prepared with 5% CdS ratio show high PL intensity with broadening peak than the sample with 20% CdS ratio indicated that it has a wide range of different particle's size distribution. Also, another peak of relatively low intensity in the range of 600 nm bears the signature of the red emission (Lambe_Klick model) [21] which could be due to the recombination of electrons trapped at sulfur (S) vacancies with valence-band-free holes.

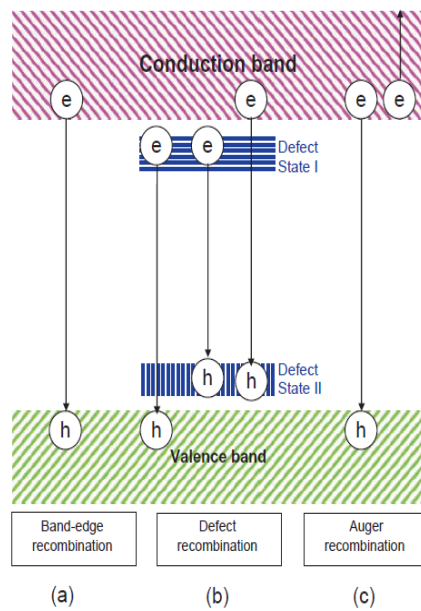


Fig. 8: A few radiative and nonradiative processes that can occur during luminescence [20]

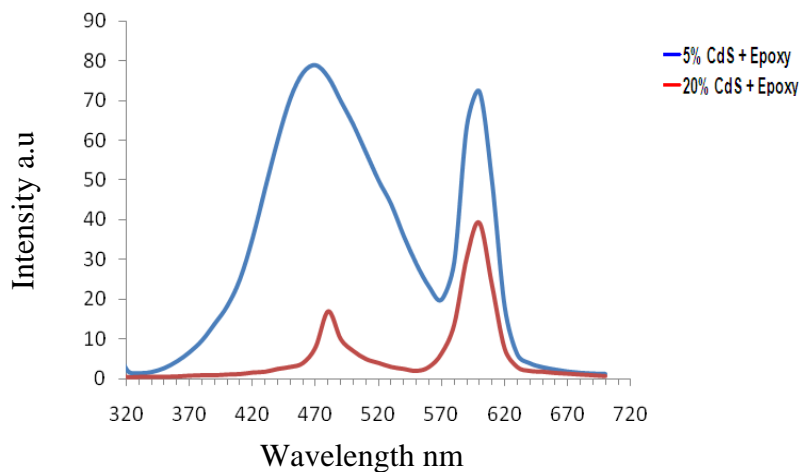


Fig. 9: PL spectra of CdS/Epoxy nanocomposites

The PL of CdS nanocrystal –polyvinylcarbazole (PVK) composites has been studied [22] for various CdS loading. The energy gap of the CdS nanoparticles in the CdS/PVK was estimated from the PL peaks to be (2.66, 2.63, 2.54, and 2.48) eV for (10, 20, 30, and 40) % CdS/PVK nanocomposites samples respectively. It has also been noted an increase in the average particle size of CdS as the CdS in the PVK increase, and a blue shift observed in the emission profile. Our PL results, however, are in a qualitative agreement with the absorbance measurements.

4. Conclusion

CdS /Epoxy nanocomposites have been synthesized using *in situ* method. The CdS nanoparticles were formed by Cd^{2+} ion and S^{2-} ion interaction in Epoxy matrix *in situ*. The optical measurements of the CdS/Epoxy nanocomposites showed a blue shifted absorption onset with respect to neat epoxy resin. The effective mass model have been used

to calculate the diameters of the CdS nanoparticles and they were 4.5 and 4.8 nm for 5% and 20% CdS+Epoxy respectively. The samples which are prepared have in the visible spectra, After 470 nm wavelength, the epoxy and the (5wt.%) CdS-epoxy samples have a high transmission (65%) but becomes of low transmittance for the (20wt.%) CdS –Epoxy sample.

The PL spectra of CdS/Epoxy showed two peaks, the first one due to energy gap variation with particle size, and the second is due to the red emission which could be due to the recombination of electrons trapped at sulfur (S) vacancies with valence-band-free holes.

References

- [1] D. Y. Godovsky, *Adv. Polym. Sci.* **159** (2000) 163
- [2] P. M. Ajayan, L. S. Schadler, P.V. Braun, *Nanocomposite Science and Technology*, Wiley VCH (2003)
- [3] H. Waad, A. Suhane, Y. Boontonngkong, C. Thanachayanout, J. Dutta, *The Third Thailand Materials Science and Technology Conference (MSAT III)*, Bangkok, pp. 16 (2004)
- [4] J. N. Hay, S. J. Shaw, *Europhysics News*, May/June (2003)
- [5] J. L. H. Chau, C.T. Tung, Yu M. Lin, A. K. Li, *Mater. Lett.* **62** (2008) 3416
- [6] N. L. D. Filho, H. A. de Aquino, *e-Polymers* **009** (2006) 1
- [7] N. D. S. Mohallem, L. M. Seara, M.A. Novak, E. H. C. P. Sinnecker, *Brazilian J. Phys.* **36** (2006) 1078
- [8] T. Mu, J. Du, Z. Li, Z. Liu, B. Han, J. Wang, D. Sun, B. Wang, *Collo. Polymer Sci.* (2004)
- [9] M. H. Ullah, J. H. Kim, C. S. Ha, *Mater. Lett.* **62** (2008) 2249
- [10] P. S. Nair, T. Radhakrishnan, N. Revaprasadu, G.A. Kolawole, *J. Mat. Sci.* **40** (2005) 4407
- [11] H. Zhang, X. Ma, D. Yang, *Mater. Lett.* **58** (2003) 5
- [12] D. Patidar, R. Sharma, N. Jain, T. P. Sharma, N. S. Saxena, *Bull. Mater. Sci.* **29** (2006) 21
- [13] Y. Q. Li, S.Y. Fu, Y. W. Mai, *Polymer* **47** (2006) 2127
- [14] J. G. Benito, *J. Coll. & Inter. Sci.* **267** (2003) 326
- [15] P. Lijia, C. Dazhu, H. Pingsheng, Z. Xino and W. Lrqian, *Mater. Reser. Bull.* **39** (2004) 243
- [16] Y. Wang, N. Herron, *Phys. Rev. B* **42** (1990) 7253
- [17] L. Brus, *J. Phys. Chem.* **90** (1986) 2555
- [18] Z. B. Sun, X. Dong, S. Shoji, X. Duan and S. Kawata, *Nanotechnology* **19** (2008) 035611
- [19] H. Wang, P. Fang, Z. Chen, S. Wang, *Appl. Surf. Sci.* **253** (2007) 8495
- [20] A. Kitai, *Luminescent Materials and Applications*, John Wiley & Sons Ltd. England (2008)
- [21] M. Karimi, M. Rabiee, F. Moztarzadeh, M. Bodaghi, M. Tahriri, *Solid State Commun.* **149** (2009) 1765
- [22] P. Chouksey, M. Tiwari, B. P. Chandra, *Int. J. Adv. Eng. & Appl.* **1** (2011) 106